Food and Chemical Toxicology 129 (2019) 1–12

Contents lists available at ScienceDirect

Food and Chemical Toxicology

journal homepage: www.elsevier.com/locate/foodchemtox

Oleuropein aglycone and hydroxytyrosol interfere differently with toxic $A\beta_{1-42}$ aggregation

Manuela Leri[a,b], Antonino Natalello[c], Elena Bruzzone[a], Massimo Stefani[a,d], Monica Bucciantini[a,d,*]

[a] Department of Biomedical, Experimental and Clinical Sciences 'Mario Serio', University of Florence, Viale Morgagni 50 - 50134, Florence, Italy
[b] Department of Neuroscience, Psychology, Area of Medicine and Health of the Child of the University of Florence, Viale Pieraccini, 6 - 50139 Florence, Italy
[c] Department of Biotechnology and Biosciences, University of Milano Bicocca, Piazza della Scienza 2, 20126, Milano, Italy
[d] Interuniversity Center for the Study of Neurodegenerative Diseases (CIMN), Florence, Italy

ARTICLE INFO

Keywords:
$A\beta_{1-42}$ peptide
Alzheimer's disease
Oleuropein aglycone
Hydroxytyrosol
Amyloid*Chemical compounds studied in this article:*
Oleuropein Aglycone (PubChem CID: 56842347)
Hydroxythyrosol (PubChem: 82755)
Dimethylsulfoxide (PubChem CID: 679)
Congo Red (PubChem CID: 11313)
MTT (PubChem CID: 64965)
Acrylamide (PubChem CID: 6579)
Sodium Dodecil Sulfate (PubChem CID: 3423265)
N,N-dimethylformamide (PubChem CID: 6228)

ABSTRACT

Oleuropein aglycone (OleA), the most abundant polyphenol in extra virgin olive oil (EVOO), and Hydroxythyrosol (HT), the OleA main metabolite, have attracted our interest due to their multitarget effects, including the interference with amyloid aggregation path. However, the mechanistic details of their anti-amyloid effect are not known yet. We report here a broad biophysical approach and cell biology techniques that enabled us to characterize the different molecular mechanisms by which OleA and HT modulate the $A\beta_{1-42}$ fibrillation, a main histopathological feature of Alzheimer's disease (AD). In particular, OleA prevents the growth of toxic $A\beta_{1-42}$ oligomers and blocks their successive growth into mature fibrils following its interaction with the peptide N-terminus, while HT speeds up harmless fibril formation. Our data demonstrate that, by stabilizing oligomers and fibrils, both polyphenols reduce their seeding activity and aggregate/membrane interaction on human neuroblastoma SH-SY5Y cells. These findings highlight the great potential of EVOO polyphenols and offer the possibility to validate and to optimize their use for possible AD prevention and therapy.

1. Introduction

Natural polyphenols are a large class of phytochemicals found in herbal beverages and in foods of plant origin. The dietary intake of flavonoids (a large class of compounds including many polyphenols) varies, from about 1.0 to 2.0 g/d, depending on the type and amount of fruit, vegetables or beverages consumed (Sandhar et al., 2011). Several animal and population studies suggest an inverse relation between a diet rich in polyphenols and the occurrence of various diseases, including cancer, cardiovascular and degenerative diseases (Valls-Pedret et al., 2012; Virmani et al., 2013). In recent years, increasing interest has been focused on plant polyphenols not only for their antioxidant properties but also due to their ability to inhibit amyloid fibril growth, to favour their disaggregation and to destabilize preformed fibrils (Stefani and Rigacci, 2013). Peptide/protein aggregation into amyloid fibrils is implicated in a number of human systemic or neurodegenerative diseases, including type 2 diabetes, Alzheimer's (AD) and Parkinson (PD) diseases. Polyphenols have also been shown to inhibit self-assembly of several peptides/proteins associated with amyloid diseases in different ways depending on the molecular features of either

Abbreviations: $A\beta_{1-42}$, peptide Aβ; OleA, Oleuropein aglycone; HT, Hydroxythyrosol; DMSO, dimethylsulfoxide; TEM, trasmission electron microscope; FBS, fetal bovine serum; DLS, Dinamic Light scattering; MTT, 3-(4,5-dimethylthiazol-2-yl)-2,5-diphenyltetrazolium bromide; CTX-B, Cholera enterotoxin subunit B; FTIR, Fourier transformed infrared; GM1, monosialotetrahexosylganglioside 1; FRET, Fluorescence Resonance Energy Transfer; Dh, hydrodynamic diameter; PBS, phosphate buffer saline; BSA, Bovine serum albumine

* Corresponding authorDepartment of Biomedical, Experimental and Clinical Sciences 'Mario Serio', University of Florence, Viale Morgagni 50, 50134, Florence, Italy.

E-mail addresses: manuela.leri@unifi.it (M. Leri), antonino.natalello@unimib.it (A. Natalello), elena.bruzzone@unifi.it (E. Bruzzone), massimo.stefani@unifi.it (M. Stefani), monica.bucciantini@unifi.it (M. Bucciantini).

https://doi.org/10.1016/j.fct.2019.04.015
Received 4 January 2019; Received in revised form 8 April 2019; Accepted 10 April 2019
Available online 14 April 2019
0278-6915/ © 2019 Published by Elsevier Ltd.

component (Ladiwala et al., 2011a,b). It has also been reported that polyphenols in the glycoside or aglycone forms act differently to remodel Aβ aggregates (Ladiwala et al., 2010).

The main phenolic compounds of extra-virgin olive oil (EVOO), a key component of the Mediterranean diet, include oleuropein aglycone (OleA) and its main metabolite, hydroxytyrosol (3,4-dihydroxyphenylethanol, HT), together with other minor components; these molecules have attracted considerable interest for their biological and pharmacological properties, including a remarkable antioxidant power (Omar, 2010; Bendini et al., 2007). Other recent data indicate that OleA interferes *in vitro* with the path of amyloid aggregation of some peptides/proteins, including amylin (Rigacci et al., 2010), the $A\beta_{1-42}$ peptide (Rigacci et al., 2011) and tau protein (Daccache et al., 2011), Transthyretin (Leri et al., 2016), β2-microglobulin (Leri et al., 2018) and α-synuclein (Palazzi et al., 2018), skipping the growth of toxic prefibrillar/oligomeric assemblies. The aggregation of tau protein was also reported to be inhibited by olive polyphenols such as oleocanthal (Daccache et al., 2011). Actually, these and other findings suggest that, at least in part, OleA protection against protein aggregation could be ascribed to its HT moiety arising from OleA hydrolysis, which occurs during drupe maturation and squeezing, EVOO storage and digestion.

The differences in the biological effects of OleA and HT remain largely elusive. Recent findings indicate that HT is the OleA moiety mostly responsible for inhibition of amylin aggregation whereas the antidiabetic effect resulting from stimulation of insulin secretion requires the whole molecule (Wu et al., 2017). Our recent data indicate the same protection by comparable doses of OleA or HT in a Tg murine model of Aβ deposition (Nardiello et al., 2018). However, reduced information and very few mechanistic data, apart those relative to the strong antioxidant power, are presently available on HT protection against AD-associated neurodegeneration (Schaffer et al., 2010).

AD is the most common form of dementia in the elderly, and its raising occurrence in developed countries, together with the lack of effective therapies, poses dramatic problems to the families of AD patients and to the national health systems. Accordingly, finding molecules or treatments useful for AD prevention and therapy or, at least, able to delay the occurrence of AD symptoms has become a largely investigated theme in biochemistry, molecular biology and pharmacology, even though the high costs and the inherent difficulties to get positive results have led some leading pharma industries to announce to stop their efforts in this research field. AD is characterized by the build-up of intracellular neurofibrillary tangles (NFTs) of hyperphosphorylated tau and of extracellular deposits of the $A\beta_{1-42}$ peptide found in diffuse and senile plaques around cerebral vessels and dystrophic/degenerating neurites (González-Correa et al., 2008). According to the amyloid cascade hypothesis (Murphy and LeVine, 2010), $A\beta_{1-42}$ and tau aggregation into oligomers and larger insoluble fibrils is heavily implicated in the neurotoxic effects observed in AD pathology (Karran et al., 2011).

Previous data on the interference of OleA with $A\beta_{1-42}$ aggregation *in vitro* and the reported beneficial effects of olive polyphenols in Aβ-exposed cells and in transgenic animal models of Aβ deposition (Nardiello et al., 2018; Irvine et al., 2008; Diomede et al., 2013; Grossi et al., 2013; Luccarini et al., 2015) prompted us to study in detail some molecular aspects of the interference of OleA and HT with $A\beta_{1-42}$ amyloid aggregation. A detailed knowledge of the molecular mechanisms underlying cytoprotection by the two polyphenols might provide significant information for future design of novel therapeutic strategies aimed at preventing, arresting and/or reversing the progression of AD and other neurodegenerative diseases with amyloid deposition.

2. Materials and methods

2.1. $A\beta_{1-42}$ aggregation

$A\beta_{1-42}$ peptide solutions were prepared by dissolving lyophilized $A\beta_{1-42}$ (Bachem, Bubendorf, Switzerland), in 100% hexafluoroisopropanol (HFIP) to a 1.0 mM final concentration. After HFIP evaporation over-night at room temperature, the samples were stored at −20 °C until use. Amyloid aggregates were grown by dissolving the peptide (25 μM final concentration) in 20 mM sodium phosphate buffer, pH 7.4, at 25 °C. These aggregation condition were compatible with the chemical and physical properties of both polyphenols. Then, the samples were sonicated for 15 min and centrifuged at $18000 \times g$ for 15 min at 4 °C; peptide concentration in the clear supernatant was determined from solution absorbance ($\varepsilon_{280} = 1490\ mol^{-1}\ cm^{-1}$). The $A\beta_{1-42}$ sample aggregated for 24 h at 25 °C without shaking was mostly populated by oligomers, whereas fibrils were mainly present in the 72 h-aged samples. $A\beta_{1-42}$ aggregation was also carried out in the presence of either 25 or 75 μM of OleA or HT (molar ratio Aβ:polyphenols = 1:1 or 1:3, respectively).

2.2. Preparation of oleuropein and hydroxytyrosol samples

Oleuropein (Extrasynthese) was deglycosylated by treatment with almond β-glucosidase (EC 3.2.1.21, Fluka, Sigma-Aldrich), as previously described (Rigacci et al., 2010, 2011). Briefly, a 10 mM solution of oleuropein in 310 μL of 0.1 M sodium phosphate buffer, pH 7.0, was incubated with 8.9 I.U. of β-glucosidase overnight at room temperature. Then, the reaction mixture was centrifuged at 18000 rpm for 10 min to precipitate OleA and the precipitate was resuspended in DMSO in 100 mM stocks. Complete oleuropein deglycosylation was confirmed by assaying the glucose released in the supernatant with the Glucose (HK) Assay kit (Sigma-Aldrich). Stocks of OleA were kept frozen and protected from light, and were used within the same day once opened.

HT was purchased from Sigma-Aldrich and the powder dissolved in aqueous solution at 100 mM final concentration and stored at −20 °C, as previously reported (Zafra-Gómez et al., 2011).

2.3. Dynamic light scattering

Dynamic light scattering (DLS) measurements were performed in a low-volume quartz cuvette (Hellma Analytics, Müllheim, Germany) using a Zetasizer Nano S DLS device from Malvern Instruments (Malvern, Worcestershire, UK) thermostated at 37 °C with a Peltier system. DLS is useful to measure the average size and size distribution of particles in solution. Size distributions by intensity and total light-scattering intensity were determined in 5 acquisitions (cell position 4.2 cm, attenuator index 7) of 10 s each, over a period of 10 min. The reported data are the average of three independent measurements.

2.4. Fourier transform infrared (FTIR) spectroscopy

The $A\beta_{1-42}$ samples at 25 μM peptide concentration in 20 mM sodium phosphate buffer, pH 7.4, were incubated at 25 °C in the absence or in the presence of OleA or HT and were analysed by FTIR spectroscopy in attenuated total reflection (ATR) at different aggregation times (24 h or 72 h). In particular, 2.0 μL sample aliquots were deposited on the diamond element of the ATR device and the spectra were collected after solvent evaporation to get a protein film (Cerf et al., 2009). Trough FTIR we can investigate the secondary structures and local conformational changes of each samples during the aggregation process. The spectra were collected and analysed as previously reported (Bisceglia et al., 2018) using a Varian 670-IR spectrometer (Varian Australia Pty Ltd, Australia) at the following conditions: 1000 scan coadditions, 25 kHz of scan speed, 2.0 cm^{-1} of spectral resolution, triangular apodization, and nitrogen-cooled Mercury Cadmium Telluride detector. Fourier self deconvolution was obtained with a full width at half height of 13.33 cm^{-1} and a resolution enhancement factor K = 1.5 (Cerf et al., 2009; Natalello et al. 2016) using the ResolutionsPro software (Varian Australia Pty Ltd, Australia).

2.5. Thioflavin T assay

To asses the amyloidogenic structure we performed a Thioflavin T (ThT) assa, a specific probe that exhibits a strong increase of its fluorescence quantum yield upon binding to cross-β-sheet structure of amyloid, thus allowing quantitative assessment of the presence of fibrillary species. . $A\beta_{1\text{-}42}$ aggregates grown for different times (0 h, 3 h, 24 h, 48 h, 72 h) in the absence or in the presence of OleA or HT, were diluted to 15 μM (monomeric peptide concentration) with 20 mM phosphate buffer, pH 7.4, at 25 °C and supplemented with a small volume of a 1.0 mM ThT solution adjusted to 20 μM final concentration. Then, each sample was transferred into multiple wells of a 96-well half-area, low-binding, clear bottom (200 μL/well) and ThT fluorescence was read at the maximum intensity of fluorescence of 485 nm using a Biotek Synergy 1H plate reader; buffer fluorescence was subtracted from the fluorescence values of all samples. To ascertain any OleA or HT interference with ThT fluorescence, controls experiments were performed where OleA and HT were added in pre-made $A\beta_{1\text{-}42}$ aggregates either immediately before or after addition of the ThT solution.

2.6. Seeding experiments

Seeding experiments were carried out using 25 μM $A\beta_{1\text{-}42}$ monomers and 72 h-aged pre-formed aggregates (F) grown in the absence or in the presence of OleA (F/OleA) or HT (F/HT), at the 1:3 protein: polyphenol molar ratio. We added seeds (at 5.0% ratio) to the monomer so that seeds concentration was 1.25 μM relative to monomer concentration (25 μM), according to Ladiwala et al., (2011).

2.7. Gel electrophoresis and silver staining

Aβ samples (25 μM, monomer concentration) aggregated for 72 h in the absence or in the presence of OleA, HT 1 × or HT 3 × were diluted in 2 × Laemmli sample buffer (Bio-Rad) and centrifuged for 20 min at 18000 × *g* at 4 °C to separate fibrils from oligomers. To analyze OleA/HT interaction with different $A\beta_{1\text{-}42}$ conformations, the samples were incubated for 3 h at 25 °C without agitation, diluited in 2 × Laemmli sample buffer (Bio-Rad) and sonicated for 1 min. Each sample was analysed using 4–20% precast Stain-Free™ gels (Bio-Rad) and silver stained.

2.8. Transmission electron microscopy (TEM) imaging

5.0 μL aliquots of $A\beta_{1\text{-}42}$ aggregated in the presence or in the absence of OleA, HT 1 × or HT 3 × , were withdrawn at different aggregation times, loaded onto a formvar/carbon-coated 400 mesh nickel grids (Agar Scientific, Stansted, UK) and negatively stained with 2.0% (w/v) uranyl acetate (Sigma-Aldrich). The grid was air-dried and examined using a JEM 1010 transmission electron microscope at 80 kV excitation voltage.

2.9. Fluorescence quenching experiments

Fluorescence quenching by acrylamide. The quenching of the tyrosine (Tyr10) emission of $A\beta_{1\text{-}42}$, which lacks tryptophan residues, was investigated with the neutral, water-soluble quencher, acrylamide. Fluorescence quenching (the decrease in intensity induced by a quencher molecule) offers a powerful approach to detect solvent exposure of Tyr10 in the monomeric, oligomeric and fibrillar $A\beta_{1\text{-}42}$. Aliquots of protein solutions were withdrawn at various aggregation times (final concentration of $A\beta_{1\text{-}42}$ 2.5 μM) and mixed with increasing concentrations of acrylamide (0–15 μM) in 20 mM sodium phosphate buffer, pH 7.4. The intrinsic fluorescence was recorded before and after addition of the quencher. The excitation wavelength was set at 275 nm and the emission intensity was scanned in the 300–450 nm range. Fluorescence intensities were corrected for dilution resulting from stepwise addition of acrylamide. Stern-Volmer plots for $A\beta_{1\text{-}42}$ were fitted with the linear equation $F0/F = Ksv^*A + q$, where *F*0 and *F* are the intrinsic fluorescence intensities in the absence and in the presence of acrylamide, respectively, A is acrylamide concentration, and *K*sv is the Stern-Volmer constant (Ladiwala et al., 2011a,b).

Fluorescence quenching by polyphenols. Aliquots of $A\beta_{1\text{-}42}$ aggregates aged 24 h were mixed with increasing OleA or HT concentrations (0–21 μM) in 20 mM phosphate buffer, pH 7.4, The curves obtained in the presence of different concentrations of polyphenols were fitted with the polynomial equation $(F0)/F = K_{sv}x^2 + K_{st}x + 1$, where *K*sv is the Stern-Volmer constant for dynamic quenching and *K*st is the static component of the quenching process (Souillac et al., 2003).

2.10. Intrinsic fluorescence measurements

Intrinsic fluorescence is a powerful indicator of protein's conformational states. Protein aromatic amino acids fluoresce upon UV excitation. During the transition of the protein from folded to unfolded states, the local environment of the aromatic amino acids also changes, which in turn affects their fluorescence properties. Intrinsic fluorescence spectra of $A\beta_{1\text{-}42}$ were collected at 275 nm excitation before and after OleA or HT supplementation and the emission intensity was scanned in the 300–430 nm range. The fluorescence emission spectra were acquired using the Biotek Synergy 1H plate reader. To perform the experiment, we analysed 25 μM $A\beta_{1\text{-}42}$ aggregates grown for 24 h in the absence or in the presence of OleA or HT after subtraction of the PBS, or polyphenols/PBS spectrum. We checked different protein:polyphenol molar ratios (1:0.5, 1:1, 1:3, 1:6 and 1:9). All samples were diluted 10 times in each reading.

2.11. Cell culture

Human neuroblastoma (SH-SY5Y) cells were cultured at 37 °C in complete medium (50% HAM, 50% DMEM, 10% foetal bovine serum, 3.0 mM glutamine, 100 units/ml penicillin and 100 μg/ml streptomycin), in a humidified, 5.0% CO_2 incubator. All materials used for cell culture were from Sigma Aldrich. To induce differentiation, 24 h after cell seeding the serum levels in the culture medium were reduced to 3.0% with 10 μM retinoic acid (RA) for seven days prior to treatment (Cheung et al., 2009). For the MTT assay, differentiated cells (RA-SH-SY5Y, 1×10^4 cells/well) were cultured in a 96-well plate. For immunofluorescence staining, the differentiated cells were cultured in a 24-well plate at 2.5×10^4 cells/well. Cell differentiation was checked by immunostaining with anti-synaptophysin antibody (Sigma-Aldrich).

2.12. MTT assay

Cell viability was assessed by the MTT assay optimized for the cell line used in the experiments. Briefly, RA-SH-SY5Y cells were seeded into 96-well plates at a density of 6000 cells/well in fresh complete medium and grown for 48 h. Then, the cells were treated for 24 h with 2.5 μM $A\beta_{1\text{-}42}$ at different times of aggregation in the presence or in the absence of OleA or HT. After 24 h of incubation, the culture medium was removed and the cells were incubated for 1.0 h at 37 °C in 100 μL of serum-free DMEM without phenol red, containing 0.5 mg/ml MTT. Then, 100 μL of cell lysis solution (20% SDS, 50% N,N-dimethylformamide) was added to each well and the samples were incubated at 37 °C for 2 h to allow complete cell lysis. The absorbance of the blue formazan resulting from MTT reduction was read at 570 nm using a spectrophotometric microplate reader. Final absorption values were calculated by averaging each sample in triplicate after blank (100 μL of MTT solution + 100 μL of lysis solution) subtraction.

2.13. ROS determination

Intracellular reactive oxygen species (ROS) were determined using

the fluorescent probe 2′,7′–dichlorofluorescein diacetate, acetyl ester (CM-H_2 DCFDA; Molecular Probes), a cell-permeant indicator for ROS that becomes-fluorescent on removal of the acetate groups by cellular esterases. The subsequent oxidation can be detected by monitoring the increase in fluorescence at 538 nm. RA-SH-SY5Y cells were plated on 96-well plates at a density of 10000 cells/well and exposed for 24 h to the aggregates. Then, 10 μM DCFDA in DMEM without phenol red was added to each well. The fluorescence values at 538 nm were detected after 30 min by Fluoroscan Ascent FL (Thermo-Fisher).

2.14. Calcium fluxes

The cytosolic levels of free Ca^{2+} were measured using the fluorescent probe Fluo-3 acetoxymethyl ester (Fluo-3 AM; Molecular Probes). Subconfluent RA-SH-SY5Y cells cultured on glass coverslips were incubated at 37 °C for 5 min with 5.0 μM Fluo-3 AM prior to exposure for different lengths of time (30 min, 1 h, 3 h or 5 h) to $A\beta_{1\text{-}42}$ aggregates grown for 72 h in the presence or in the absence of OleA, HT 1 × or HT 3 × . At the end of the incubation, the cells were fixed in 2.0% buffered paraformaldehyde for 10 min. Cell fluorescence was imaged using a confocal Leica TCS SP5 scanning microscope (Leica, Mannheim, Ge) equipped with a HeNe/Ar laser source for fluorescence measurements. The observations were performed using a Leica Plan 7 Apo X63 oil immersion objective, suited with optics for DIC acquisition. Cells from five independent experiments and three areas (about 20 cells/area) per experiment were analysed. Fluorescence intensity of Fluo3-AM was measured using the ImageJ software (National Institutes of Health Bethesda, MD), and expressed as arbitrary units.

2.15. Immunofluorescence

Subconfluent RA-SH-SY5Y cells grown on glass coverslips were exposed for 24 h to 2.5 μM $A\beta_{1\text{-}42}$ aggregates grown in the presence or in the absence of polyphenols (OleA, HT 1 × or HT 3 ×) and then washed with PBS. GM1 labelling was performed by incubating the cells with 10 ng/mL CTX-B Alexa488 in complete medium for 10 min at room temperature. Then, the cells were fixed in 2.0% buffered paraformaldehyde for 10 min and permeabilized by treatment with a 1:1 acetone/ethanol solution for 4.0 min at room temperature, washed with PBS and blocked with PBS containing 0.5% BSA and 0.2% gelatin. After incubation for 1.0 h at room temperature with rabbit anti-$A\beta_{1\text{-}42}$ polyclonal antibody diluted 1:600 in blocking solution, the cells were washed with PBS for 30 min under stirring and then incubated with Alexa568-conjugated anti-rabbit secondary antibody (Molecular Probes) diluted 1:100 in PBS. Finally, the cells were washed twice in PBS and once in distilled water to remove non-specifically bound antibodies. Cell fluorescence was imaged using a confocal Leica TCS SP5 scanning microscope (Leica, Mannheim, Ge) equipped with a HeNe/Ar laser source for fluorescence measurements. The observations were performed using a Leica Plan 7 Apo X63 oil immersion objective. FRET analysis was performed by adopting the FRET sensitized emission method, as previously reported (Nosi et al., 2012).

2.16. Statistical analysis

Statistical analysis of the data was performed by using one way analysis of variance (ANOVA).

3. Results

3.1. Biophysical features of $A\beta_{1\text{-}42}$ aggregates

Initially, we investigated the role of OleA or HT in $A\beta_{1\text{-}42}$ aggregation, by carrying out a ThT binding assay using two different protein/polyphenols molar ratios (1:1 and 1:3). We investigated this range to compare our data with previously reported findings relative to

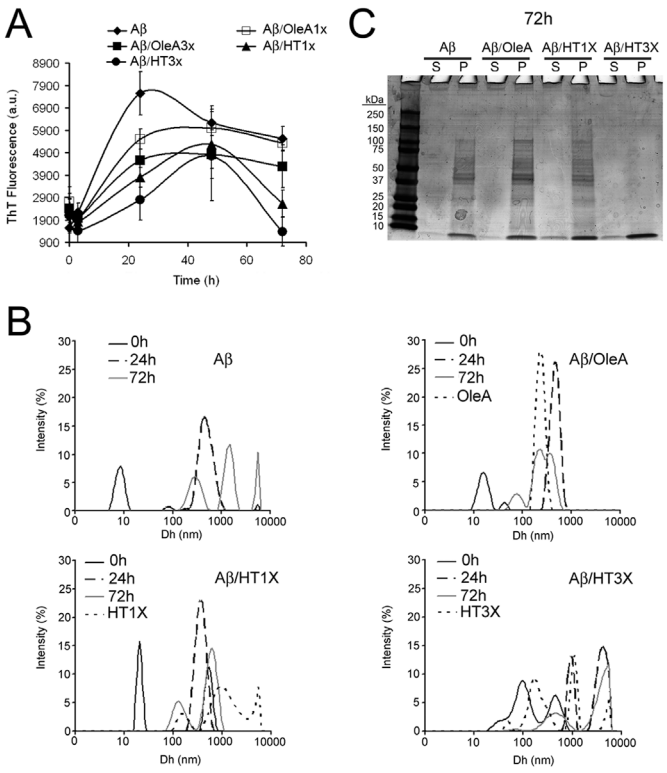

Fig. 1. Biophysical analysis of $A\beta_{1-42}$ aggregation. (**A**) ThT fluorescence intensity of the samples aggregated in the absence (♦) or in the presence of OleA or HT: OleA 1x (□), OleA 3 × (■), HT 1 × (▲), HT 3 × (●) recorded at different times of aggregation (0 h, 24 h, 48 h and 72 h). (**B**) DLS spectra of $A\beta_{1\text{-}42}$ aggregates grown in the presence or in the absence of OleA or HT under the same conditions. (**C**) SDS-Page of aggregates aged 72 h in the presence or in the absence of OleA and HT 1 × or HT 3 × . The MW of the protein standards span from 250 KDa to 10 KDa.

$A\beta_{1\text{-}42}$ aggregation under different conditions (Rigacci et al., 2011). Therefore, we used $A\beta_{1\text{-}42}$ (25 μM) mixed with 25 μM (1:1 M ratio; 1 ×) and 75 μM (1:3 M ratio; 3 ×) of OleA or HT. The best protein/polyphenols molar ratio was determined by assessing the effects of either polyphenol on $A\beta_{1\text{-}42}$-induced toxicity on exposed human RA-SH-SY5Y neuroblastoma cells using the 3-(4,5-dimethylthiazol-2-yl)-2,5-diphenyltetrazolium bromide (MTT) reduction assay (Supplementary Fig. 1). These preliminary data showed that for OleA the 1:3 M ratio was the concentration that induced a total recovery of cell viability (Supplementary Fig. 1B) and the higher reduction of ThT fluorescence (Fig. 1A). The same molar ratio was used for HTTwo concentrations 1:1 and 1:3 were used for HT, to compare the OleA and HT effects (Supplementary Fig. 1A and 1A); in addition, to assess whether the biological efficacy was due to OleA or to its metabolite, we used also the 1:1 M ratio considering that about 30% of OleA is metabolised to HT (Santos et al., 2012). The samples were made to aggregate at 25 °C without shaking (see under Material and Methods), then, aliquots were withdrawn at different times of aggregation and analysed. Fig. 1A reports the maximum fluorescence intensity at 485 nm resulting from ThT binding to $A\beta_{1\text{-}42}$ at different times of aggregation (0–72 h) in the presence or in the absence of either polyphenol. The maximum intensity of fluorescence was recorded after 24 h of aggregation, followed by a progressive decrease. In the presence of OleA and HT, we recorded a reduction of total ThT fluorescence intensity at each time; in particular, a remarkable reduction of the maximum fluorescence intensity (around 40%) was seen. These data suggest either reduced aggregation, thus confirming previous data with OleA (Rigacci et al., 2010, 2011; Leri et al., 2016, 2018) and/or the growth, during aggregation, of intermediate and fibrillar species with reduced affinity to ThT respect to

that displayed by the species grown in the absence of either polyphenol. In the Aβ/OleA samples, a plateau was observed after 24 h of incubation while in the Aβ/HT samples the maximum fluorescence intensity was reached after about 48 h of incubation, followed by a drastic reduction.

To monitor particle size distribution at different times of aggregation, the same samples were also analysed by DLS after centrifugation at 14000 rpm at 4 °C to spin down large aggregates. Small species with a hydrodynamic diameter (D_h) of around 8.0 nm were found in the protein sample before starting aggregation (0 h). Oligomers with D_h around 300 nm were found in the sample after 24 h of aggregation and heterogeneous materials including oligomers and fibrils around 200, 1000 e 6000 nm in size were detected after 72 h (Fig. 1B). At the same aggregation times but in the presence of OleA, the average particle size of the aggregated material was slightly larger than that measured for aggregates grown in the absence of OleA (at 0 h and 24 h), while it appeared reduced in the 72 h aged sample (Fig. 1B). When the same experiments were carried out in the presence of two different concentrations of HT, at each time point we found a dose-dependent, yet moderate, growth of larger species indicating faster aggregation (Fig. 1B).

Finally, the sizes of the $A\beta_{1\text{-}42}$ aggregates grown for 72 h in the absence or in the presence of OleA, HT 1 × or HT 3 × were analysed by SDS-page after separation of soluble (oligomers) from insoluble aggregates by centrifugation. We found that SDS affected differently the aggregates grown in the presence of HT 3 × respect to those grown alone or in the presence of OleA or of HT 1 × (Fig. 1C). In fact, the aggregates grown in the presence of HT 3 × appeared completely dissolved by SDS, suggesting reduced stability of these larger aggregates.

Taken together, the findings of the ThT, DLS and SDS-PAGE analysis suggest that both polyphenols interfere, although differently, with the path of $A\beta_{1\text{-}42}$ aggregation. In fact, OleA favours the growth of minute protofibrils inhibiting their further growth along the fibrillation path, in agreement with our previous data (Rigacci et al., 2011), whereas HT favours the growth of $A\beta_{1\text{-}42}$ oligomers into higher Mw species with biophysical properties different from those of the aggregates arising from $A\beta_{1\text{-}42}$ alone. To extend these data we carried out further analysis of the structural and morphological features of the aggregates grown under the conditions reported above.

3.2. Structural and morphological analysis of $A\beta_{1\text{-}42}$ aggregates

Once described $A\beta_{1\text{-}42}$ aggregation and aggregate stability at different aggregation times in the absence or in the presence of either polyphenol, we investigated the structural features of the aggregates. The $A\beta_{1\text{-}42}$ secondary structure at different aggregation times (24 h or 72 h) in the absence or in the presence of OleA or HT was investigated by ATR-FTIR spectroscopy (Fig. 2A). The Fourier self deconvoluted spectrum of the peptide incubated for 24 h under aggregation conditions displayed two Amide I components around 1693 cm^{-1} and 1629 cm^{-1} previously proposed as the spectral signature of the oligomeric $A\beta_{1\text{-}42}$ peptide (Cerf et al., 2009). In particular, the two components were assigned to anti-parallel β-sheet structures in oligomeric and amorphous aggregates of $A\beta_{1\text{-}42}$ (Cerf et al., 2009) and other peptides (Sarroukh et al., 2013; Natalello et al., 2008). Similar spectral features were observed when $A\beta_{1\text{-}42}$ was aggregated in the presence of OleA or HT, suggesting that 24 h of aggregation under these conditions results in the massive presence of oligomeric species and/or immature fibrils. At prolonged times of aggregation (72 h), the intensity of the ~1693 cm^{-1} component clearly decreased in the spectra of $A\beta_{1\text{-}42}$ aggregated in the presence or in the absence of HT 1 × or HT 3 × , and the Amide I band of these samples was dominated by the component at ~1629 cm^{-1}. These results suggest a structural transition from antiparallel to parallel β-sheet in peptide fibrils (Cerf et al., 2009). On the contrary, the ~1693 cm^{-1} component remained more evident in the presence of OleA, suggesting that the latter while not inhibiting the

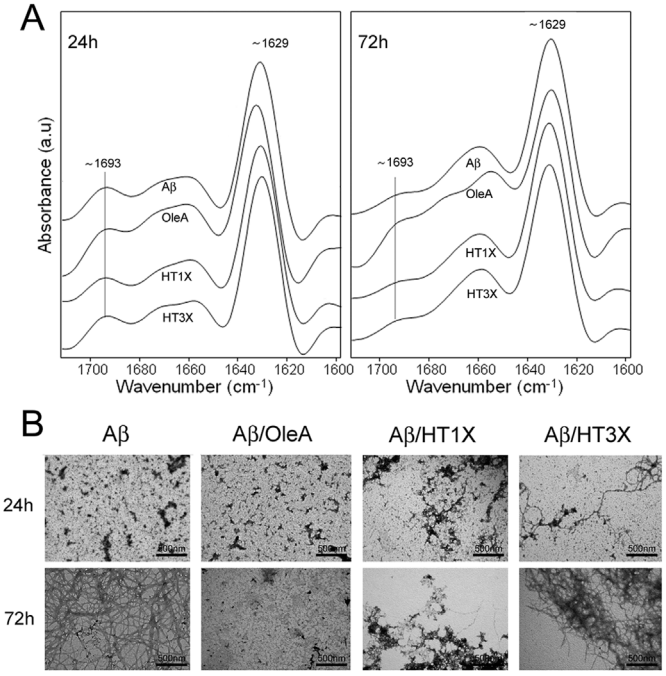

Fig. 2. Morphological and secondary structures analysis of $A\beta_{1\text{-}42}$ aggregates obtained in the presence or in the absence of polyphenols. (**A**) Fourier self deconvoluted ATR-FTIR spectra of $A\beta_{1\text{-}42}$ incubated for 24 h or 72 h in the presence or in the absence of OleA, HT 1 × , or HT 3 × . The ~1629 cm^{-1} and ~1693 cm^{-1} components are indicated. The spectra are partially superimposed and shifted along the y axis for better visualization. (**B**) TEM images of $A\beta_{1\text{-}42}$ aggregated for 24 h or 72 h in the presence or in the absence of OleA, HT 1 × or HT 3 × .

growth of oligomeric species hindered that of mature fibrils. Overall, these data agree with the biophysical characterization and confirm that HT favours the growth of fibrils, yet with different structural features.

The structural features of the assemblies populating the different steps of fibrillogenesis in the absence or in the presence of OleA or HT were further investigated by TEM. Only oligomeric and pre-fibrillar structures were evident in the $A\beta_{1\text{-}42}$ sample aggregated for 24 h in the absence or in the presence of the polyphenols (Fig. 2B), confirming previous findings with OleA (Rigacci et al., 2010). The samples grown in the presence of HT (1 × or 3 ×) were enriched in short linear protofibrils. After prolonged incubation (72 h), packed dense clusters of mature fibrils were observed in $A\beta_{1\text{-}42}$ aggregated alone or in the presence of HT 3 × ; both fibrils and prefibrillar structures were populated in the sample aggregated in the presence of HT 1 × , whereas the fibrillar species were still completely absent in the sample aggregated in the presence of OleA (Fig. 2B). Overall, these data confirm that OleA hinders potently the growth of mature fibrils while stabilizing prefibrillar species enriched in antiparallel β-sheet, whereas HT seems to accelerate the formation of ThT-negative and SDS-soluble fibrils with antiparallel β-sheet structure, as shown by the FTIR analysis reported above. The results obtained with OleA are comparable to those previously reported for tau (Daccache et al., 2011), amylin (Rigacci et al., 2010) and transthyretin (Leri et al., 2016) and confirm our previous findings obtained with a higher OleA:Aβ ratio (Rigacci et al., 2011).

3.3. OleA and HT interaction with $A\beta_{1\text{-}42}$

To better describe the structural modifications in $A\beta_{1\text{-}42}$ aggregates grown in the presence of either polyphenol, we performed quenching experiments of $A\beta_{1\text{-}42}$ intrinsic fluorescence in the presence of acrylamide. In particular, we analysed solvent exposure and intrinsic fluorescent property of Tyr10 that is completely exposed in the oligomeric

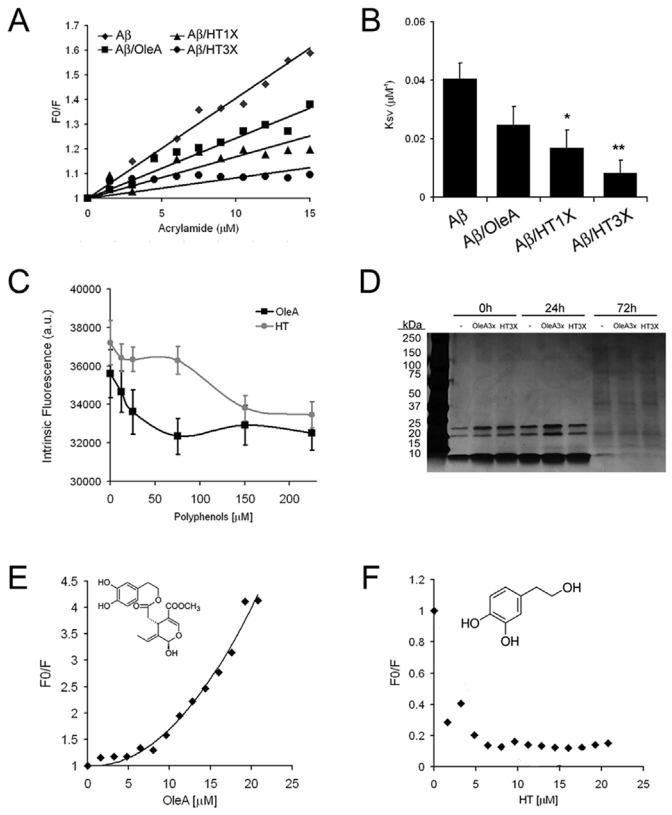

Fig. 3. OleA selectively interacts with the fraction enriched in $A\beta_{1\text{-}42}$ oligomers. (**A**) Stern-Volmer quenching plot of $A\beta_{1\text{-}42}$ grown for 24 h in the absence or in the presence of either polyphenol. (**B**) Stern-Volmer quenching constant (Ksv) ± SD calculated from the linear fit of the data in (**A**). (**C**) Intensity of intrinsic fluorescence emission of $A\beta_{1\text{-}42}$ aggregates aged 24 h as a function of OleA or HT concentration. (**D**) SDS-page of the fractions enriched in monomer (0 h), oligomers (24 h) and fibrils (72 h), after incubation for 3 h with OleA or HT. (**E, F**) Intrinsic fluorescence quenching induced by OleA (**E**) or HT (**F**) in 24 h-aged $A\beta_{1\text{-}42}$ aggregates grown in the absence of polyphenols. *$p < 0.05$; **$p < 0.01$ respect to $A\beta_{1-42}$ alone.

species while it is significantly buried in mature fibrils, in accordance with its proximity to the cross-β core (Aran Terol et al., 2015). We found that the Stern-Volmer plots were linear with oligomers growth after 24 h of aggregation (Fig. 3A), in agreement with the addition of a collisional quencher such as acrylamide (Eftink and Ghiron, 1976). However, the acrylamide quenching effects were significantly reduced (by about 10%, 50% and 60%, respectively) in the same aggregates grown in the presence of OleA, HT 1 × or HT 3 × , as indicated by the Stern-Volmer quenching constants (K_{sv}) (Fig. 3B), suggesting increasingly reduced exposure of this residue.

To extend these data, we also analysed the intrinsic fluorescence of 25 μM $A\beta_{1\text{-}42}$ aggregated for 24 h in the presence of different concentrations of either OleA or HT (at 0 × , 0.5 × , 1 × , 3 × , 6 × and 9 × respect to $A\beta_{1\text{-}42}$ M concentration). Fig. 3C shows that OleA interfered with Tyr10 exposure already at the lowest concentrations (0.5 × , 1 × , 3 ×) in a dose-dependent manner, whereas the $A\beta_{1\text{-}42}$ intrinsic fluorescence did not change in the presence of the same concentrations of HT; rather, for HT the highest concentrations tested (6 × and 9 ×) were required to produce similar effects. The low acrylamide quenching observed in Fig. 3A and the lack of modifications of intrinsic fluorescence intensity in $A\beta_{1\text{-}42}$ grown in the presence of low concentrations of HT suggest reduced solvent exposure of Tyr10. Overall, in addition to the TEM and FTIR analysis, our data, indicate that HT activates the fibrillation process of $A\beta_{1\text{-}42}$, whereas OleA stabilizes the oligomeric intermediates that exhibit solvent-exposed Tyr10 thus significantly delaying fibril formation. Next, we sought to assess whether the two polyphenols were also able to bind pre-formed aggregates and to identify, if any, the specific amyloid assembly they interacted with. To do this, we performed SDS-page analysis of $A\beta_{1\text{-}42}$ conformers populated in peptide samples aggregated for 0, 24 or 72 h and then treated for 3 h with or without 3 × OleA or HT. We found that the two polyphenols did not bind mature fibrils populating the 72 h-aged $A\beta_{1\text{-}42}$ sample; rather, they interacted with the $A\beta_{1\text{-}42}$ sample aged 0 h or 24 h, mainly populated by monomers and oligomers; moreover, during the incubation time with the polyphenols (3 h) we observed that the SDS-resistant intermediates with a molecular weight around 25 kDa were stabilized (Fig. 3D). These results are not surprising; in fact, it has been reported that other polyphenols do interact with amyloid structures in a conformation-, rather than sequence-dependent mode (Yang et al., 2005).

To confirm that OleA interacted specifically with the $A\beta_{1\text{-}42}$ species arising from 24 h-aggregation, we used OleA and HT as Tyr10 quenchers. Fig. 3E shows the Stern-Volmer plot of Tyr10 quenching by OleA. The polynomial fitting suggests that OleA, due to its higher than HT hydrophobicity, contacted more easily the exposed aromatic residues of the peptide. Moreover, the fitting indicates that OleA, at the lowest dose, interacted specifically with aromatic residues by static quenching, whereas a dynamic quenching was observed with progressive saturation of protein binding sites. These data support the possibility that OleA interferes with $A\beta_{1\text{-}42}$ aggregation in two different, yet not mutually exclusive, ways: i) by binding the monomeric peptide and ii) by binding the nascent aggregates, thus generating complexes with different aggregation propensities. Moreover, as expected, the lack of quenching by HT indicated that the latter, much more hydrophilic than OleA, interacted with $A\beta_{1\text{-}42}$ aggregates in a completely different manner (Fig. 3F). Indeed, at all concentrations tested, HT interacted negligibly with exposed aromatic residues in 24 h-aged aggregates, suggesting that HT bind to $A\beta_{1\text{-}42}$ in a different region respect to OleA.

3.4. Biochemical modifications in aggregate-exposed cells

Once described the interference of either polyphenol with the aggregation path of $A\beta_{1\text{-}42}$ together with the different interaction mode with the peptide, we investigated whether, and to what extent, OleA or HT affected the cytotoxicity of $A\beta_{1-42}$ aggregates. To do this, we treated RA-SH-SY5Y neuroblastoma cells for 24 h with 2.5 μM (monomer concentration) $A\beta_{1-42}$ aggregates grown in the absence or in the presence of OleA or HT 1 × or 3 × . At the end of the incubation, cell viability was assayed by the MTT test. The $A\beta_{1\text{-}42}$ aggregates aged 24 h or 72 h displayed similar cytotoxicity, reducing cell viability by about 40% and 50%, respectively whereas the polyphenols did not exhibit any intrinsic cytotoxicity (Fig. 4A); however, aggregate toxicity was reduced similarly when the cells were exposed to the same concentrations of $A\beta_{1\text{-}42}$ aggregates grown 24 h or 72 h in the presence of OleA or HT. In particular, cell viability recovery was about 20% ± 7.8% in the presence of $A\beta_{1-42}$ -OleA and 30% ± 9.0% in the presence of $A\beta_{1-42}$ -HT 1 × or 3 × (Fig. 4A); the latter figure indicates greater efficacy of HT respect to Ole against aggregate cytotoxicity. Similar data were obtained with 72 h-aged aggregates grown in the presence of OleA or HT.

Then, we investigated the protection mechanisms by OleA and HT against β-amyloid-induced cytotoxicity. It is known that Ca^{2+} and ROS derangement are important biochemical and functional modifications underlying cytotoxicity to aggregate-exposed cells (Bucciantini et al., 2004; Novitskaya et al., 2006); accordingly, we checked whether OleA and HT were protective against $A\beta_{1-42}$ aggregate toxicity in terms of Ca^{2+} and ROS levels. We measured intracellular free Ca^{2+} (Fig. 4C and D) and ROS (Fig. 4B) by using the fluorescent probes Fluo-3-acetoxymethyl ester (Fluo-3AM) and CM-H_2DCFDA, respectively. As expected, ROS levels were increased by 1.5 and 2.5 fold in cells exposed to 24 h- or 72 h-aged $A\beta_{1\text{-}42}$ aggregates with respect to untreated cells. However, the oxidative stress was reduced in cells exposed to amyloid

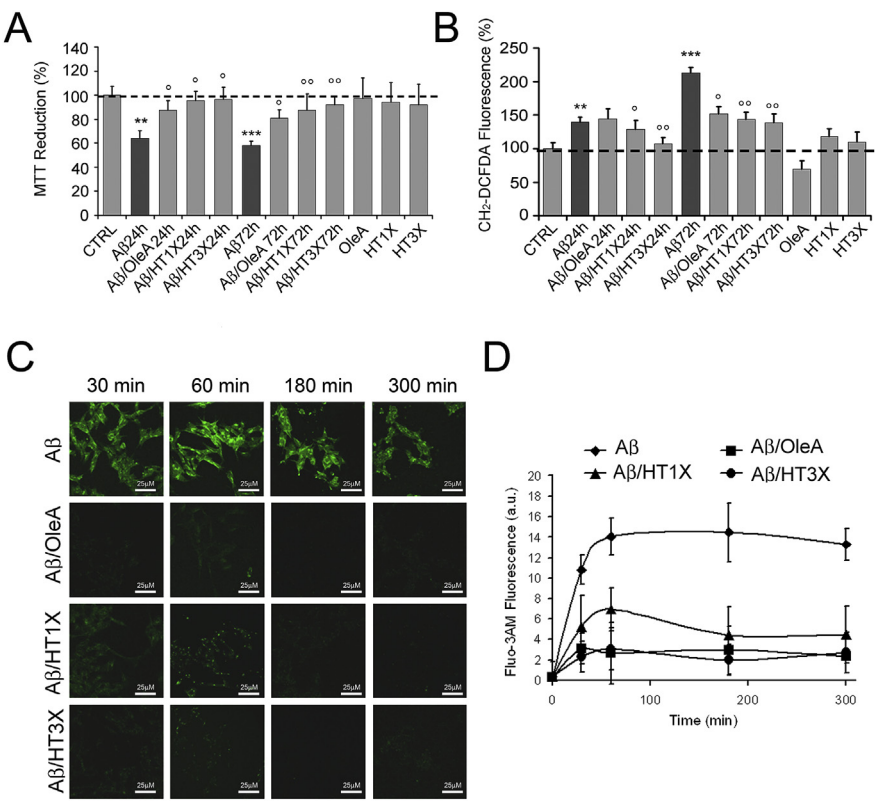

Fig. 4. Cytotoxicity of $A\beta_{1-42}$ aggregates. RA-SH-SY5Y cells exposed for 24 h to 2.5 μM (monomer concentration) $A\beta_{1-42}$ samples previously aggregated for 24 h or 72 h in the absence or in the presence of OleA ($A\beta_{1-42}$/OleA), HT 1 × ($A\beta_{1-42}$/HT 1 ×) or HT 3 × ($A\beta_{1-42}$/HT 3 ×). (**A**) MTT assay (**B**) ROS production in RA-SH-SY5Y cells exposed for 24 h to the same aggregates. (**C**) Confocal microscopy imaging of intracellular free Ca^{2+} levels in RA-SH-SY5Y cells exposed for 30 min, 1 h, 3 h or 5 h to 2.5 μM $A\beta_{1-42}$ aggregated for 72 h in the absence or in the presence of OleA 3 × (Aβ/OleA), HT1 × (Aβ/HT 1 ×) or HT 3 × (Aβ/HT 3 ×). (**D**) Quantification of Fluo-3AM fluorescence intensity. Error bars indicate the standard error of three independent experiments carried out in triplicate. **p < 0.01; ***p < 0.001 vs control. p < 0.05; p < 0.01 vs $A\beta_{1-42}$ aggregates.

aggregates grown in the presence of either polyphenol. This effect was particularly evident in cells exposed to fibrils-enriched $A\beta_{1-42}$ samples grown in the presence of OleA and even more evident in cells exposed to $A\beta_{1-42}$ aggregates grown in the presence of HT. It is unlikely that the higher HT efficacy against oxidative stress in aggregate-exposed cells was due to its stronger anti-oxidant power, as the same protection was recorded in cells exposed to the aggregates grown in the presence of either 1 × or 3 × HT [40, 41], in agreement with our previous data in OleA-fed CRND8 mice (Grossi et al., 2013; Luccarini et al., 2015).

Finally, we measured the intracellular free Ca^{2+} levels in RA-SH-SY5Y cells exposed to $A\beta_{1-42}$ aggregated for 24 h (data not shown) or 72 h in the absence or in the presence of OleA or HT. Fig. 4C and D shows a time-dependent increase of the intracellular Ca^{2+} level in cells exposed to 2.5 μM $A\beta_{1-42}$ aggregated for 72 h (the same increase of Ca^{2+} levels was found in cells exposed to 24 h-aged aggregates). However, we did not observe any significant increase of intracellular Ca^{2+} in cells treated with the same concentration of $A\beta_{1-42}$ aggregates grown in the presence of OleA, HT 1 × or HT 3 × , in agreement with the MTT and ROS data. Overall, our findings besides confirming previous data relative to OleA (Grossi et al., 2013; Luccarini et al., 2015), indicate that HT is also able to reduce the cytotoxicity of $A\beta_{1-42}$ aggregates both in their fibrillar and pre-fibrillar conformations relieving, even more efficiently than OleA, the amyloid-induced increase of Ca^{2+} influx and ROS production. We did not investigate the molecular mechanisms underlying OleA and HT protection against oxidative stress and Ca^{2+} increase; therefore, we cannot exclude that either polyphenol reaches these effects by affecting different cellular functions.

3.5. Interaction of $A\beta_{1-42}$ aggregates with the cell membrane

It is widely reported that amyloid aggregate cytotoxicity requires the primary interaction of the amyloids with the cell membrane; the latter results in functional and/or structural perturbation of the membrane with ensuing derangement of cell signalling (Silva et al., 2006; Cicerale et al., 2012; Bucciantini et al., 2012; Calamai and Pavone, 2013) and alterations of free Ca^{2+} and ROS levels (Bucciantini et al., 2004; Pellistri et al., 2008). Other effects, such as the interaction with membrane receptors (Pellistri et al., 2008; Salazar and Strittmatter, 2017; Haas and Strittmatter, 2016; Abedini et al., 2018) and the interference with signalling pathways have also been reported (.Haas and Strittmatter, 2016; Zhang et al., 2008). Accordingly, we sought to relate protection by either polyphenol against aggregate cytotoxicity to the ability of the different $A\beta_{1-42}$ aggregates grown in the absence or in the presence of OleA or HT to interact with the cell membrane of the exposed cells. To do this, we performed confocal microscopy experiments using both a polyclonal antibody raised against recombinant $A\beta_{1-42}$ and Alexa 488-conjugated CTX-B. The latter is a probe specific for the monosialotetrahexosylganglioside 1 (GM1), a common lipid raft marker widely reported as an important interaction site for amyloids (Bucciantini et al., 2012; Evangelisti et al., 2012; Hong et al., 2014).

Confocal imaging showed that $A\beta_{1-42}$ aggregates built up at the RA-SH-SY5Y plasma membrane (Fig. 5). These aggregates not only co-localized with GM1 in general terms but also displayed FRET signal suggesting their close spatial relation or even direct interaction with membrane GM1 (Fig. 5, panel a). However, when the cells were exposed to the much less toxic $A\beta_{1-42}$ aggregates grown in the presence of OleA or HT, we did not observe any aggregate cluster on the membrane and consequently, any FRET signal with GM1 (Fig. 5, panels 2c, 3c, 4c). These data confirm the importance of aggregate-membrane interaction as a trigger of cell toxicity and provide a rationale for the lack of cytotoxicity of the aggregates grown in the presence of either polyphenol.

3.6. Self-propagation of $A\beta_{1-42}$ aggregates grown in the presence of OleA or HT

Neurodegenerative diseases are characterized by self-propagation of pre-formed aggregates by secondary nucleation. Several studies report data showing that fibrillar material extracted from brain tissue of AD people accelerates fibril growth from $A\beta_{1-42}$ *in vitro*, and that synthetic fibrils are able to seed further fibril growth (Petkova et al., 2005;

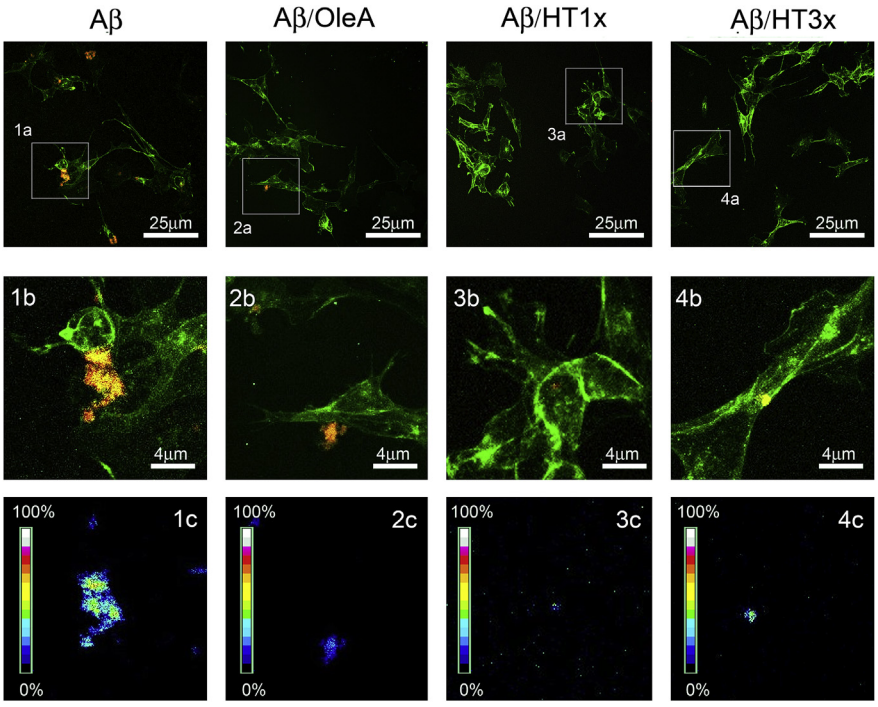

Fig. 5. Immunolocalization of $A\beta_{1\text{-}42}$ aggregates on the plasma membrane. RA-SH-SY5Y cells exposed for 24 h to 2.5 μM (monomer concentration) $A\beta_{1\text{-}42}$ aggregated for 72 h in the absence (lane 1) or in the presence (lane 2; Aβ/OleA) of OleA, of HT 1 × (lane 3; Aβ/HT 1 ×) or HT 3 × (lane 4; Aβ/HT 3 ×). The cells were stained with Alexa 488-conjugated CTX-B (green fluorescence); protein aggregates were stained with anti-$A\beta_{1\text{-}42}$ antibodies followed by treatment with Alexa 568-conjugated anti-rabbit secondary antibodies (red fluorescence). Channels merge is shown in panels **a**. Panels **b** show magnifications of selected areas in panels **a**. FRET efficiency is shown in panels **c** for aggregates grown 72 h in the absence (**1c**, Aβ) or in the presence (**2c**, Aβ/OleA) of 3 × OleA, of HT 1 × (**3c**, Aβ/HT 1 ×) or of HT 3 × (**4c**, Aβ/HT 3 ×), respectively. (For interpretation of the references to colour in this figure legend, the reader is referred to the Web version of this article.)

Paravastu et al., 2009). This aspect is very important for disease outcome, considering that seeding worsens AD severity. On the basis of these data, we sought to determine whether $A\beta_{1\text{-}42}$ aggregates grown in the absence or in the presence of either polyphenol displayed the same seeding ability. The data reported above showed that the secondary structure of aggregates grown in the presence of OleA or HT was similar to that displayed by $A\beta_{1-42}$ aggregated in the absence of either polyphenol, even though with different structural/morphological features and reduced cytotoxicity (Figs. 2 and 4).

We first used ThT assay (Fig. 6A) and TEM imaging (Fig. 6B) to evaluate the seeding ability (5% seed to monomeric $A\beta_{1\text{-}42}$) of 72 h-aged $A\beta_{1-42}$ fibrillar (F) aggregates grown in the absence or in the presence of OleA (F/OleA) or HT (F/HT). We observed that, in the first 24 h of aggregation, $A\beta_{1\text{-}42}$ fibrils favoured amyloid aggregation acting as seeds when monomeric $A\beta_{1-42}$ was present in solution (Aβ + F), as indicated by the higher ThT fluorescence intensity with respect to unseeded $A\beta_{1\text{-}42}$ (Aβ, Fig. 6A). We did not investigate whether the increased fibrillation resulted from secondary nucleation, however this observation agrees with previous results indicating that pre-formed fibrils are able to seed monomers with fibrillar conformation (Paravastu et al., 2009; Langer et al. 2011). On the contrary, we did not find any seeding ability of F/OleA or F/HT; moreover, in this case, the aggregation path was different and its extent was reduced, as indicated by an extended lag phase and by a reduced ThT fluorescence intensity (Fig. 6A). These results were confirmed by TEM images (Fig. 6B) showing that $A\beta_{1\text{-}42}$ seeding with F/OleA populated mostly ThT-negative oligomeric assemblies, whereas long and well-structured fibrils were seen in unseeded 24 h-aged $A\beta_{1\text{-}42}$ or in 24 h-aged $A\beta_{1\text{-}42}$ seeded with F, (Fig. 6B). When $A\beta_{1\text{-}42}$ was seeded under the same conditions with F/HT, fibrillar structures morphologically different from those found in the Aβ + F samples were observed (Fig. 6B).

We also checked the cytotoxicity of the seeded samples to RA-SH-SY5Y cells. The results reported in Fig. 6C indicate that the Aβ + F/OleA or Aβ + F/HT aggregates were significantly less toxic than both Aβ + F and 24 h aged $A\beta_{1\text{-}42}$ samples, with a significant recovery of vitality by ~50%. In these cells, we also observed a remarkable reduction of oxidative stress to levels comparable to those recorded in control cells (Fig. 6D). Finally, these results were confirmed by immunofluorescence experiments, showing that only a few Aβ + F/OleA or Aβ + F/HT aggregates were found on the cell membrane that exhibited the same FRET efficiency with the cell membrane GM1 (Fig. 6E).

4. Discussion

Amyloid diseases, most of which are associated with increased ageing of the population, are a major burden to public health. In particular, type 2 diabetes and neurodegenerative diseases such as Alzheimer's and Parkinson's diseases are remarkably increasing in developed countries and pose a severe challenge to families and healthcare systems. For example, Alzheimer's disease, whose prevalence progressively increases with age (from 4% among people < 65 years, to over 13% in the > 65-year age-group, and up to 50% in the > 85-year age-group), is a severe healthcare burden with epidemic proportions in the USA, where it is the fifth leading cause of death in people older than 65 years (Alzheimer's Association. Alzheimer's Association Report Alzheimer's Disease Facts and Fig. 2007. www.alz.org/national/documents/PR_FFfactsheet.pdf) and other developed countries. It is estimated that there are currently 36 million people with AD worldwide and by 2050, that figure is projected to grow to AD-diagnosed 106 million; therefore, accelerated development of effective therapies against amyloid diseases is strongly needed. However, due to the high costs of research and development, some leading pharma industries have recently announced stop to the investments in research on Alzheimer's and Parkinson's diseases, further increasing the interest in research on nutraceuticals.

In this study, we focused our attention on the ability of EVOO polyphenols, OleA and HT, to interact with amyloid aggregates, inhibiting fibril or steering oligomer growth into unstructured, non-toxic species.

Recent studies indicate that several small aromatic molecules interfere with amyloid aggregation, possibly by remodelling the amyloid intermediates through different mechanisms of interactions (Bastianetto and Quirion, 2004; Pawar et al., 2005) or, rather than inhibiting, by redirecting or speeding up the aggregation cascade towards non-toxic species (Necula et al., 2007; Wang et al., 2008; Lee et al., 2006; Blanchard et al., 2004).

Our findings suggest two different mechanisms by which the main EVOO polyphenols interfere with Aβ aggregation. Our ThT and FTIR

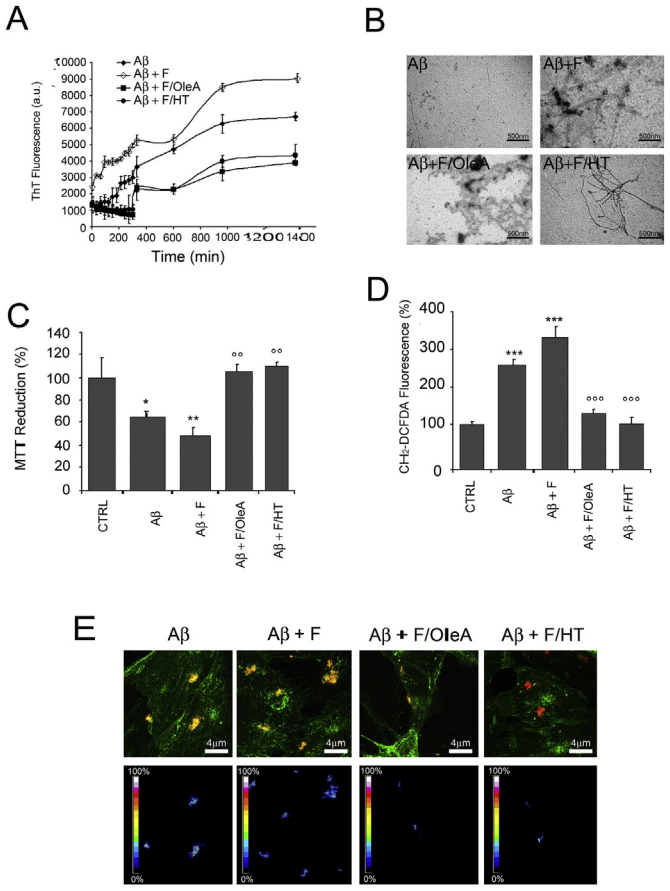

Fig. 6. Aggregation kinetics of seeded $A\beta_{1\text{-}42}$ fibrils and their cytotoxicity. 72 h-aged $A\beta_{1\text{-}42}$ fibrils (F) grown in the absence or in the presence of OleA (F/OleA) or HT (F/HT), were used as seeds and added to monomeric $A\beta_{1\text{-}42}$. Aβ: monomeric $A\beta_{1\text{-}42}$ after 24 h of aggregation in the absence of seeds. Aβ + F: monomeric $A\beta_{1\text{-}42}$ aggregated 24 h in the presence of seeds of 72 h-aged $A\beta_{1\text{-}42}$. Aβ + F/OleA: $A\beta_{1\text{-}42}$ aggregated 24 h in the presence of pre-formed 72 h-aged $A\beta_{1\text{-}42}$ -OleA seeds. Aβ + F/HT: $A\beta_{1\text{-}42}$ aggregated 24 h in the presence of pre-formed 72 h-aged $A\beta_{1\text{-}42}$ –HT seeds. (**A**) ThT fluorescence intensity recorded at different times of aggregation. (**B**) TEM images (**C**) MTT assay and (**D**) ROS production in RA-SH-SY5Y cells exposed for 24 h to the different $A\beta_{1\text{-}42}$ samples at a final concentration of 2.5 μM (monomer concentration). (**E**) Confocal microscopy imaging (top) and FRET efficiency (bottom) in RA-SH-SY5Y cells exposed to different $A\beta_{1\text{-}42}$ aggregates seeded with different seeds (at 5% seed/monomer ratio). Error bars indicate the standard error of three independent experiments carried out in triplicate. **p < 0.01; ***p < 0.001 vs control. °p < 0.05; °p < 0.01 vs 24 h $A\beta_{1\text{-}42}$ aggregates.

data agree with previous findings indicating that the interaction between the phenolic ring in polyphenols and the aromatic residues in amyloidogenic proteins prevents π-π interactions thus disturbing π-stacking between protein units blocking self-assembly into amyloid fibrils (Cheng et al., 2013). In particular, the intrinsic fluorescence analysis of $A\beta_{1\text{-}42}$ after 24 h of aggregation in the presence of different OleA concentrations (Fig. 3C) and the dose-dependent quenching effects of OleA on pre-formed $A\beta_{1\text{-}42}$ aggregates aged 24 h (Fig. 3E) indicated that the Tyr10 residue could be involved in the interaction with the phenolic rings in OleA.

Our data agree with previous NMR and mass spectrometry studies showing that OLE interacts, non-covalently, in a (1:2) stoichiometry with $A\beta_{1\text{-}42}$ mainly at the peptide N-terminus (4–11), in addition to the (12–22) and (17–28) regions (Galanakis et al., 2011; Bazoti et al., 2008). Recently, some reports implicating the "N-Terminal Hypothesis" for AD, highlighted the importance of the contact between the $A\beta_{1\text{-}42}$ flexible N-terminus and its central hydrophobic core to form a double-hairpin in toxic $A\beta_{1\text{-}42}$ oligomers and fibrils (Das et al., 2015; Wälti et al., 2016; Hoyer et al., 2008). Recent studies have also reported the involvement of the N-terminal residues Arg5, Asp7 and Ser8 in fibrils stabilization (Murray et al., 2017; Söldner et al., 2017). Finally, the $A\beta_{1\text{-}42}$ N-terminus has been also suggested to be crucial in binding to the cell membrane (Urbanc et al., 2011), some receptors (Kam et al., 2013) and for neurotoxicity. Overall, these data support the importance of the $A\beta_{1\text{–}42}$ N-terminus as a molecular target to develop aggregation inhibitors for therapeutic purposes.

In this context, our results suggest a modulatory activity of OleA that results in prevention of the growth of toxic $A\beta_{1\text{–}42}$ oligomers and blocks their successive growth into mature fibrils following the primary interaction with the N-terminus of the monomeric and/or oligomeric peptide. These effects affected peptide cytotoxicity; in fact, the amyloid assemblies grown in the presence of OleA exhibited poor cytotoxicity (Fig. 5) mainly as a consequence of their inability to bind the cell membrane at the GM1 level, as indicated by FRET efficiency data (Fig. 6).

To better understand the molecular mechanism underlying the interference of OleA with $A\beta_{1\text{-}42}$ aggregation we also took into consideration the effects of HT, its polyphenol moiety arising from enzymatic hydrolysis of OleA and its glycoside in the mature drupe or in the stomach (Corona et al., 2006). HT, a strong antioxidant, has been found in the brain of OleA-fed CRND8 mice, a model of $A\beta_{1\text{-}42}$ deposition (Luccarini et al., 2015), were it has been found to elicit the same protective effects of the whole OleA molecule (Nardiello et al., 2018). We therefore analysed the effects of HT on $A\beta_{1\text{-}42}$ aggregation to provide support to the reported protection against cognitive deficits in HT-fed mice and to assess whether such protection involved similar molecular mechanisms. We found that HT, differently from OleA, accelerated fibrils formation. Its different action on the aggregation path of $A\beta_{1\text{-}42}$ could be due to its increased hydrophilic character and to its inability to act as quencher of $A\beta_{1\text{-}42}$ intrinsic fluorescence (Fig. 3F). We also noticed that the final aggregation products grown in the presence of 3 × HT did not bind ThT and were SDS-sensitive (Fig. 1), though still displaying amyloid secondary structure, as shown by the FTIR data (Fig. 2A). It is possible that HT interacts with hydrophobic residues in the central region of Aβ42 peptides leading to more efficient intermolecular interactions and aggregation. HT is an aromatic compound that can potentially form π-stacking interactions with the hydrophobic residues of Phe19 and Phe20, previously shown to be critical for efficient amyloid polymerization *in vitro* of Aβ42 (Kumar et al., 2015). HT could also promote the off-pathway aggregation of Aβ42 via alternative hydrogen bonding facilitated by the presence of several hydroxyl groups.

The observation that OleA and HT act differently is not surprising, since different polyphenols and other low molecular weight molecules have been reported to inhibit amyloid aggregation by interacting with different monomeric, oligomeric or fibrillar conformations (Ladiwala et al., 2010). In some cases, the appearance of oligomeric species can be inhibited while fibril growth is promoted, in other cases, fibril, but not oligomer, growth or, alternatively, both oligomer and fibril growth, is inhibited (Taniguchi et al., 2005; Berhanu and Masunov, 2010; Ehrnhoefer et al., 2008). However, the fluorescence assay did not allow us to ascertain whether HT and OleA interacted with monomeric or oligomeric Aβ or with more complex aggregates. Yet, our data lead us to propose some mechanisms (which do not exclude each other): (i) monomeric Aβ that convert to a β-sheet conformation are scavenged by the polyphenols thus reducing the number of aggregation-prone hydrophobic monomers and nucleation sites in the solution, and reducing the number of toxic oligomers, (ii) the polyphenols stabilize the oligomers, thus slowing down their conversion to fibrils, (iii) the polyphenols bind the monomeric or oligomeric peptide favouring the presence of aggregation-prone conformations inside non-toxic and more-complex aggregates.

Recent data have shown that amyloid aggregation of $A\beta_{1\text{-}42}$ can be

influenced by peptide post-translational modification. Phosphorylation and oxidation events have been involved in β-sheet stabilization, increasing peptide fibrillation and reducing its relative cytotoxicity (Kumar and Walter, 2011; Misiti et al., 2010; Clementi et al., 2006). Considering that the antioxidant activity transforms HT into a catechol quinone (Rietjens et al., 2007), these aspects induced us to hypothesize that HT could increase fibrils formation by inducing some chemical modification of the aggregate surface. The latter can be a very important issue considering that the aggregation kinetics depend on sequence-specific features including secondary structure preferences, hydrophobicity, stability, and net charge (Chiti et al., 2003). We are currently investigating the chemical modification hypothesis through a deeper structural analysis of the aggregates grown in the presence of HT.

Seeding of aggregate growth by pre-formed aggregates through secondary nucleation has repeatedly been reported (Paravastu et al., 2009; Langer et al., 2011). Recent data indicate that monomer polymerization and aggregation in the presence of seeds is important for amyloid toxicity (Jan et al., 2010) and that it is at the basis of the progressive spreading of the pathology associated to several amyloid forming proteins (Jucker and Walker, 2011) including Aβ (Aguzzi et al., 2007; Langer et al., 2011; Lee et al., 2010) and α-synuclein (Luk et al., 2012; Volpicelli-Daley et al., 2011). Accordingly, we studied the seeding activity of the aggregates grown in the absence or in the presence of OleA or HT. We observed that the fibrils grown in the presence of OleA showed a remarkable reduction of seeding activity on monomeric $A\beta_{1-42}$ peptide, such that no fibril formation was ascertained under these conditions. Furthermore, the few small oligomeric and prefibrillar-like species found in the $A\beta_{1\text{-}42}$ sample seeded with preformed fibrils grown in the presence of OleA were still able to bind to the cell membrane but their toxicity was substantially abolished. The seeds of $A\beta_{1\text{-}42}$ aggregates grown in the presence of HT induced the formation of fibril-like aggregates generally cross-linked and thinner than those grown in the absence of the polyphenol. These aggregates were less able to bind ThT and, also in this case, did not increase ROS production nor they reduced viability in exposed cells.

The differences in the aggregation and seeding kinetics of $A\beta_{1\text{-}42}$ in the absence or in the presence of either polyphenol support the notion that the intricate process of $A\beta_{1\text{-}42}$ fibrillation is determined by multiple factors; they also indicate that the different conformational structures arising in the presence of OleA or HT critically affect the properties of $A\beta_{1\text{-}42}$ fibrils. Overall, our data suggest that the main EVOO polyphenols interfere remarkably with the fibrillar aggregation, aggregate seeding and cytotoxicity of $A\beta_{1\text{-}42}$. Furthermore OleA and HT hinder $A\beta_{1\text{-}42}$ cytotoxicity in a linear manner, as shown by the MTT assay dose-dependence (Supplementary Fig. 1) only at the lower protein:polyphenols molar ratio (up to 1:1 for HT and 1:3 for OleA). This observation suggests that low level of polyphenol are sufficient to induce specific and essential changes in the monomeric peptide or oligomeric assemblies to redirect the aggregation process toward off-pathway and harmless final products. We can suppose that, in the presence of polyphenols peptide fibrillation proceeds through an heterogeneous nucleation step where new aggregates are generated in the presence of polyphenols, as previously reported for other molecules and for cholesterol (Habchi et al., 2018).

These data are of interest if we consider bioavailability and metabolism of OleA and HT, quite complex and not completely described processes that include the participation of the gut microbiota and depend on a number of factors, including gender, the form in which they are ingested, dosing, duration of the treatment, and association with different foods. (de Bock, et al., 2013). Accordingly, definitive conclusions on polyphenols, including OleA and HT, bioavailability are difficult to obtain (D'Archivio et al. 2010; Angeloni et al., 2017), so that it is not easy to get solid information on their plasma and tissue concentrations. Some results support the view that secoiridoids aglycones are better absorbed than their glycated counterparts and suggest that the EVOO matrix contributes to phenols stability in the gastrointestinal tract and favours their absorption. Particularly relevant in the context of AD is the experimental evidence suggesting that, in rat and in humans, orally-administered OleA and HT cross the blood-brain barrier (BBB) and are found inside brain parenchyma (Serra et al., 2012; Vissers et al., 2002; Nardiello et al., 2018). This imply that under conditions of regular intake, even low amounts of OleA and HT can be adsorbed, with increase of their plasma and cellular concentration. Finally, OleA and HT hydrophobicity favours their interaction with cell membranes (Paiva-Martins et al., 2010), which implies their build-up at the cellular level, where they can reach local concentrations higher than in plasma.

This conclusion highlights the great potential of these molecules or their molecular scaffolds, to develop novel drugs to prevent Aβ pathology and/or to hinder its spreading and relieve its neurotoxic effects thus reducing neurodegeneration at different stages of AD progression.

Acknowledgments

This project was supported by Ente Cassa di Risparmio di Firenze [N° 2015.1002A2202.3931]. M.L. was supported by ANCC-COOP/Airalzh ONLUS [Reg. n° 0043966.30-10- 359 2014-u] through University of Florence [D.R.595/2016].

Appendix A. Supplementary data

Supplementary data to this article can be found online at https://doi.org/10.1016/j.fct.2019.04.015.

References

Abedini, A., Derk, J., Schmidt, A.M., 2018. The receptor for advanced glycation end-products is a mediator of toxicity by IAPP and other proteotoxic aggregates: establishing and exploiting common ground for novel amyloidosis therapies. Protein Sci. 27 (7), 1166–1180.

Aguzzi, A., Heikenwalder, M., Polymenidou, M., 2007. Insight into prions strains and neurotoxicity. Nat. Rev. Mol. Cell Biol. 8 (7), 552–561 (submitted for publication).

Alzheimer's Association, 2007. Alzheimer's association report Alzheimer's disease facts and figures. www.alz.org/national/documents/PR_FFfactsheet.pdf.

Angeloni, C., Malaguti, M., Barbalace, M.C., Hrelia, S., 2017. Bioactivity of olive oil phenols in neuroprotection. Int. J. Mol. Sci. 18, 2230.

Aran Terol, P., Kumita, J.R., Hook, S.C., Dobson, C.M., Esbjörner, E.K., 2015. Solvent exposure of Tyr10 as a probe of structural differences between monomeric and aggregated forms of the amyloid-β peptide. Biochem. Biophys. Res. Commun. 468 (4), 696–701.

Bastianetto, S., Quirion, R., 2004. Natural antioxidants and neurodegenerative diseases. Front. Biosci. 9, 3447–3452.

Bazoti, F.N., Bergquist, J., Markides, K., Tsarbopoulos, A., 2008. Localization of the noncovalent binding site between amyloid-beta-peptide and oleuropein using electrospray ionization FT-ICR mass spectrometry. J. Am. Soc. Mass Spectrom. 8, 1078–1085.

Bendini, A., Cerretani, L., Carrasco-Pancorbo, A., Gómez-Caravaca, A.M., Segura-Carretero, A., Fernández-Gutiérrez, A., Lercker, G., 2007. Phenolic molecules in virgin olive oils: a survey of their sensory properties, health effects, antioxidant activity and analytical methods: an overview of the last decade. Molecules 12, 1679–1719.

Berhanu, W.M., Masunov, A.E., 2010. Natural polyphenols as inhibitors of amyloid aggregation. Molecular dynamics study of GNNQQNY heptapeptide decamer. Biophys. Chem. 149, 12–21.

Bisceglia, F., Natalello, A., Serafini, M.M., Colombo, R., Verga, L., Lanni, C., De Lorenzi, E., 2018. An integrated strategy to correlate aggregation state, structure and toxicity of Aβ1–42 oligomers. Talanta 188, 17–26.

Blanchard, B.J., Chen, A., Rozeboom, L.M., Stafford, K.A., Weigele, P., Ingram, V.M., 2004. Efficient reversal of Alzheimer's disease fibril formation and elimination of neurotoxicity by a small molecule. Proc. Natl. Acad. Sci. U.S.A. 101, 14326–14332.

Bucciantini, M., Calloni, G., Chiti, F., Formigli, L., Nosi, D., Dobson, C.M., Stefani, M., 2004. Prefibrillar amyloid protein aggregates share common features of cytotoxicity. J. Biol. Chem. 279 (30), 31374–31382.

Bucciantini, M., Nosi, D., Forzan, M., Russo, E., Calamai, M., Pieri, L., Formigli, L., Quercioli, F., Soria, S., Pavone, F., Savistchenko, J., Melki, R., Stefani, M., 2012. Toxic effects of amyloid fibrils on cell membranes: the importance of ganglioside GM1. FASEB J. 26 (2), 818–831.

Calamai, M., Pavone, F.S., 2013. Partitioning and confinement of GM1 ganglioside induced by amyloid aggregates. FEBS Lett. 587, 1385–1391.

Cerf, E., Sarroukh, R., Tamamizu-Kato, S., Breydo, L., Derclaye, S., Dufrêne, Y.F., Narayanaswami, V., Goormaghtigh, E., Ruysschaert, J.M., Raussens, V., 2009.

Antiparallel beta-sheet: a signature structure of the oligomeric amyloid beta-peptide. Biochem. J. 421 (3), 415–423.
Cheng, B., Gong, H., Xiao, H., Petersen, R.B., Zheng, L., Huang, K., 2013. Inhibiting toxic aggregation of amyloidogenic proteins: a therapeutic strategy for protein misfolding diseases. Biochim. Biophys. Acta 1830, 4860–4871.
Cheung, Y.T., Lau, W.K., Yu, M.S., Lai, C.S., Yeung, S.C., So, K.F., Chang, R.C., 2009. Effects of all-trans-retinoic acid on human SH-SY5Y neuroblastoma as in vitro model in neurotoxicity research. Neurotoxicology 30 (1), 127–135.
Chiti, F., Stefani, M., Taddei, N., Ramponi, G., Dobson, C.M., 2003. Rationalization of the effects of mutations on peptide and protein aggregation rates. Nature 424 (6950), 805–808.
Cicerale, S., Lucas, L.J., Keast, R.S., 2012. Antimicrobial, antioxidant and anti-inflammatory phenolic activities in extra virgin olive oil. Curr. Opin. Biotechnol. 23 (2), 129–135.
Clementi, M.E., Pezzotti, M., Orsini, F., Sampaolese, B., Mezzogori, D., Grassi, C., Giardina, B., Misiti, F., 2006. Alzheimer's amyloid beta-peptide (1-42) induces cell death in human neuroblastoma via bax/bcl-2 ratio increase: an intriguing role for methionine 35. Biochem. Biophys. Res. Commun. 342, 206–213.
Corona, G., Tzounis, X., Assunta Dessì, M., Deiana, M., Debnam, E.S., Visioli, F., Spencer, J.P., 2006. The fate of olive oil polyphenols in the gastrointestinal tract: implications of gastric and colonic microflora-dependent biotransformation. Free Radic. Res. 40 (6), 647–658.
D'Archivio, M., Filesi, C., Varì, R., Scazzocchio, B., Masella, R., 2010. Bioavailability of the polyphenols: status and controversies. Int. J. Mol. Sci. 11 (4), 1321–1342.
Daccache, A., Lion, C., Sibille, N., Gerard, M., Slomianny, C., Lippens, G., Cotelle, P., 2011. Oleuropein and derivatives from olives as Tau aggregation inhibitors. Neurochem. Int. 58 (6), 700–707.
Das, P., Murray, B., Belfort, G., 2015. Alzheimer's protective A2T mutation changes the conformational landscape of the Aβ1−42 monomer differently than does the A2V mutation. Biophys. J. 108 (3), 738–747.
de Bock, M., Thorstensen, E.B., Derraik, J.G., Henderson, H.V., Hofman, P.L., Cutfield, W.S., 2013. Human absorption and metabolism of oleuropein and hydroxytyrosol ingested as olive (Olea europaea L.) leaf extract. Mol. Nutr. Food Res. 57, 2079–2085.
Diomede, L., Rigacci, S., Romeo, M., Stefani, M., Salmona, M., 2013. Oleuropein aglycone protects transgenic C. elegans strains expressing Aβ42 by reducing plaque load and motor deficit. PLoS One 8 (3), e58893.
Eftink, M.R., Ghiron, C.A., 1976. Exposure of tryptophanyl residues in proteins. Quantitative determination by fluorescence quenching studies. Biochemistry 15 (3), 672–680.
Ehrnhoefer, D.E., Bieschke, J., Boeddrich, A., Herbst, M., Masino, L., Lurz, R., Engemann, S., Pastore, A., Wanker, E.E., 2008. EGCG redirects amyloidogenic polypeptides into unstructured, off-pathway oligomers. Nat. Struct. Mol. Biol. 15, 558–566.
Evangelisti, E., Cecchi, C., Cascella, R., Sgromo, C., Becatti, M., Dobson, C.M., Chiti, F., Stefani, M., 2012. Membrane lipid composition and its physicochemical properties define cell vulnerability to aberrant protein oligomers. J. Cell Sci. 125, 2416–2427.
Galanakis, P.A., Bazoti, F.N., Bergquist, J., Markides, K., Spyroulias, G.A., Tsarbopoulos, A., 2011. Study of the interaction between the amyloid beta peptide (1-40) and antioxidant compounds by nuclear magnetic resonance spectroscopy. Biopolymers 96, 316–327.
González-Correa, J.A., Navas, M.D., Lopez-Villodres, J.A., Trujillo, M., Espartero, J.L., De La Cruz, J.P., 2008. Neuroprotective effect of hydroxytyrosol and hydroxytyrosol acetate in rat brain slices subjected to hypoxia-reoxygenation. Neurosci. Lett. 446 (2–3), 143–146.
Grossi, C., Rigacci, S., Ambrosini, S., Ed Dami, T., Luccarini, I., Traini, C., Failli, P., Berti, A., Casamenti, F., Stefani, M., 2013. The polyphenol oleuropein aglycone protects TgCRND8 mice against Aß plaque pathology. PLoS One 8 (8), e71702.
Haas, L.T., Strittmatter, S.M., 2016. Oligomers of amyloid β prevent physiological activation of the cellular prion protein-metabotropic glutamate receptor 5 complex by glutamate in Alzheimer disease. J. Biol. Chem. 291 (33), 17112–17121.
Habchi, J., Chia, S., Galvagnion, C., Michaels, T.C.T., Bellaiche, M.M.J., Ruggeri, F.S., et al., 2018. Cholesterol catalyses Aβ42 aggregation through a heterogeneous nucleation pathway in the presence of lipid membranes. Nat. Chem. 10, 673.
Hong, S., Ostaszewski, B.L., Yang, T., O'Malley, T.T., Jin, M., Yanagisawa, K., Li, S., Bartels, T., Selkoe, D.J., 2014. Soluble Aβ oligomers are rapidly sequestered from brain ISF in vivo and bind GM1 ganglioside on cellular membranes. Neuron 82, 308–319.
Hoyer, W., Grönwall, C., Härd, T., 2008. Stabilization of a β-hairpin in monomeric Alzheimer's amyloid-β peptide inhibits amyloid formation. Proc. Natl. Acad. Sci. U.S.A. 105, 5099–5104.
Irvine, G.B., El-Agnaf, O.M., Shankar, G.M., Walsh, D.M., 2008. Protein aggregation in the brain: the molecular basis for Alzheimer's and Parkinson's diseases. Mol. Med. 14 (7–8), 451–464.
Jan, A., Hartley, D.M., Lashuel, H.A., 2010. Preparation and characterization of toxic Abeta aggregates for structural and functional studies in Alzheimer's disease research. Nat. Protoc. 5 (6), 1186–1209.
Jucker, M., Walker, L.C., 2011. Pathogenic protein seeding in Alzheimer's disease and other neurodegenerative disorders. Ann. Neurol. 70, 532–540.
Kam, T.I., Song, S., Gwon, Y., Park, H., Yan, J.J., Im, I., Choi, J.W., Choi, T.Y., Kim, J., Song, D.K., Takai, T., Kim, Y.C., Kim, K.S., Choi, S.Y., Choi, S., Klein, W.L., Yuan, J., Jung, Y.K., 2013. FcγRIIb mediates amyloid-β neurotoxicity and memory impairment in Alzheimer's disease. J. Clin. Investig. 123, 2791–2802.
Karran, E., Mercken, M., De Strooper, B., 2011. The amyloid cascade hypothesis for Alzheimer's disease: an appraisal for the development of therapeutics. Nat. Rev. Drug Discov. 10, 698–712.
Kumar, S., Walter, J., 2011. Phosphorylation of amyloid beta (Aβ) peptides – a trigger for formation of toxic aggregates in Alzheimer's disease. Aging (Albany NY) 3 (8), 803–812.
Kumar, J., Namsechi, R., Sim, V.L., 2015. Structure-based peptide design to modulate amyloid beta aggregation and reduce cytotoxicity. PLoS One 10 (6), e0129087.
Ladiwala, A.R., Dordick, J.S., Tessier, P.M., 2011a. Aromatic small molecules remodel toxic soluble oligomers of amyloid beta through three independent pathways. J. Biol. Chem. 286, 3209–3218.
Ladiwala, A.R., Lin, J.C., Bale, S.S., Marcelino-Cruz, A.M., Bhattacharya, M., Dordick, J.S., 2011b. Resveratrol selectively remodels soluble oligomers and fibrils of amyloid Abeta into off-pathway. Resveratrol selectively remodels soluble oligomers and fibrils of amyloid Abeta into off-pathway conformers. J. Biol. Chem. 286 (5), 3209–3218.
Ladiwala, A.R., Mora-Pale, M., Lin, J.C., Bale, S.S., Fishman, Z.S., Dordick, J.S., Tessier, P.M., 2010. Polyphenolic glycosides and aglycones utilize opposing pathways to selectively remodel and inactivate toxic oligomers of amyloid β. Chembiochem 12, 1749–1758.
Langer, F., Eisele, Y.S., Fritschi, S.K., Staufenbiel, M., Walker, L.C., Jucker, M., 2011. Soluble Aβ seeds are potent inducers of cerebral β-amyloid deposition. J. Neurosci. 31 (41), 14488–14495.
Lee, C.H., Kim, H.J., Lee, J.H., Cho, H.J., Kim, J., Chung, K.C., Jung, S., Paik, S.R., 2006. Dequalinium-induced protofibril formation of alpha-synuclein. J. Biol. Chem. 281, 3463–3472.
Lee, S.J., Desplats, P., Sigurolson, C., Tsigelny, I., Masliah, E., 2010. Cell-to-cell transmission of non prion protein aggregates. Nat. Rev. Neurol. 6, 702–706.
Leri, M., Nosi, D., Natalello, A., Porcari, R., Ramazzotti, M., Chiti, F., Bellotti, V., Doglia, S.M., Stefani, M., Bucciantini, M., 2016. The polyphenol Oleuropein aglycone hinders the growth of toxic transthyretin amyloid assemblies. J. Nutr. Biochem. 30, 153–166.
Leri, M., Oropesa-Nuñez, R., Canale, C., Raimondi, S., Giorgetti, S., Bruzzone, E., Bellotti, V., Stefani, M., Bucciantini, M., 2018. Oleuropein aglycone: a polyphenol with different targets against amyloid toxicity. Biochim. Biophys. Acta 1862 (6), 1432–1442.
Luccarini, I., Grossi, C., Rigacci, S., Coppi, E., Pugliese, A.M., Pantano, D., la Marca, G., Ed Dami, T., Berti, A., Stefani, M., Casamenti, F., 2015. Oleuropein aglycone protects against pyroglutamylated-3 amyloid-ß toxicity: biochemical, epigenetic and functional correlates. Neurobiol. Aging 36 (2), 648–663.
Luk, K.C., Kehm, V.M., Zhang, B., O'Brien, P., Trojanowski, J.Q., Lee, V.M., 2012. Intracerebral inoculation of pathological α-synuclein initiates a rapidly progressive neurodegeneration α-synucleinopathy in mice. J. Exp. Med. 209, 975–986.
Misiti, F., Clementi, M.E., Giardina, B., 2010. Oxidation of methionine 35 reduces toxicity of the amyloid beta-peptide(1-42) in neuroblastoma cells (IMR-32) via enzyme methionine sulfoxide reductase A expression and function. Neurochem. Int. 56 (4), 597–602.
Murphy, M.P., LeVine 3rd, H., 2010. Alzheimer's disease and the amyloid-beta peptide. J. Alzheimer's Dis. 19 (1), 311–323.
Murray, B., Sharma, B., Belfort, G., 2017. N-terminal hypothesis for Alzheimer's disease. ACS Chem. Neurosci. 8 (3), 432–434.
Nardiello, P., Pantano, D., Lapucci, A., Stefani, M., Casamenti, F., 2018. Diet supplementation with hydroxytyrosol ameliorates brain pathology and restores cognitive functions in a mouse model of amyloid-β deposition. J. Alzheimer's Dis. 63, 1161–1172.
Natalello, A., Mangione, P.P., Giorgetti, S., Porcari, R., Marchese, L., Zorzoli, I., Relini, A., Ami, D., Faravelli, G., Valli, M., Stoppini, M., Doglia, S.M., Bellotti, V., Raimondi, S., 2016. Co-fibrillogenesis of wild-type and D76N β2-microglobulin: the crucial role of fibrillar seeds. J. Biol. Chem. 291 (18), 9678–9689.
Natalello, A., Prokorov, V.V., Tagliavini, F., Morbin, M., Forloni, G., Beeg, M., Manzoni, C., Colombo, L., Gobbi, M., Salmona, M., Doglia, S.M., 2008. Conformational plasticity of the gerstmann–Sträussler–Scheinker disease peptide as indicated by its multiple aggregation pathways. J. Mol. Biol. 381, 1349–1361.
Necula, M., Kayed, R., Milton, S., Glabe, C.G., 2007. Small molecule inhibitors of aggregation indicate that amyloid beta oligomerization and fibrillization pathways are independent and distinct. J. Biol. Chem. 282, 10311–10324.
Nosi, D., Mercatelli, R., Chellini, F., Soria, S., Pini, A., Formigli, L., Quercioli, F., 2012. A molecular imaging analysis of Cx43 association with Cdo during skeletal myoblast differentiation. J. Biophot. 6, 612–621.
Novitskaya, V., Bocharova, O.V., Bronstein, I., Baskakov, I.V., 2006. Amyloid fibrils of mammalian prion protein are highly toxic to cultured cells and primary neurons. J. Biol. Chem. 281, 13828–13836.
Omar, S.H., 2010. Oleuropein in olive and its pharmacological effects. Sci. Pharm. 78, 133–154.
Palazzi, L., Bruzzone, E., Bisello, G., Leri, M., Stefani, M., Bucciantini, M., Polverino de Laureto, P., 2018. Oleuropein aglycone stabilizes the monomeric α-synuclein and favours the growth of non-toxic aggregates. Sci. Rep. 8 (1), 8337.
Paiva-Martins, F., Fernandes, J., Santos, V., Silva, L., Borges, F., Rocha, S., et al., 2010. Powerful protective role of 3,4-dihydroxyphenylethanol-elenolic acid dialdehyde against erythrocyte oxidative-induced hemolysis. J. Agric. Food Chem. 58 (1), 135–140.
Paravastu, A.K., Qahwash, I., Leapman, R.D., Meredith, S.C., Tycko, R., 2009. Seeded growth of β-amyloid fibrils from Alzheimer's brain-derived fibrils produces a distinct fibril structure. Proc. Natl. Acad. Sci. U.S.A. 106 (18), 7443–7448.
Pawar, A.P., Dubay, K.F., Zurdo, J., Chiti, F., Vendruscolo, M., Dobson, C.M., 2005. Prediction of "aggregation-prone" and "aggregation-susceptible" regions in proteins associated with neurodegenerative diseases. J. Mol. Biol. 350, 379–392.
Pellistri, F., Bucciantini, M., Relini, A., Nosi, D., Gliozzi, A., Robello, M., Stefani, M., 2008. Nonspecific interaction of prefibrillar amyloid aggregates with glutamatergic receptors results in Ca2+ increase in primary neuronal cells. J. Biol. Chem. 283 (44), 29950–29960.
Petkova, A.T., Leapman, R.D., Guo, Z., Yau, W.M., Mattson, M.P., Tycko, R., 2005. Self-propagating, molecular-level polymorphism in Alzheimer's beta-amyloid fibrils.

Science 307, 262–265.
Rietjens, S.J., Bast, A., de Vente, J., Haenen, G.R., 2007. The olive oil antioxidant hydroxytyrosol efficiently protects against the oxidative stress-induced impairment of the NObullet response of isolated rat aorta. Am. J. Physiol. Heart Circ. Physiol. 292 (4), H1931–H1936.
Rigacci, S., Guidotti, V., Bucciantini, M., Nichino, D., Relini, A., Berti, A., Stefani, M., 2011. Aβ(1-42) aggregates into non-toxic amyloid assemblies in the presence of the natural polyphenol oleuropein aglycon. Curr. Alzheimer Res. 8 (8), 841–852.
Rigacci, S., Guidotti, V., Bucciantini, M., Parri, M., Nediani, C., Cerbai, E., Stefani, M., Berti, A., 2010. Oleuropein aglycon prevents cytotoxic amyloid aggregation of human amylin. J. Nutr. Biochem. 21, 726–735.
Salazar, S.V., Strittmatter, S.M., 2017. Cellular prion protein as a receptor for amyloid-β oligomers in Alzheimer's disease. Biochem. Biophys. Res. Commun. 483 (4), 1143–1147.
Sandhar, H.K., Kumar, B., Prasher, S., Tiwari, P., Salhan, M., Sharma, P., 2011. A review of phytochemistry and pharmacology of flavonoids. Int. Pharm. Sci. 1, 25–41.
Santos, M.M., Piccirillo, C., Castro, P.M.L., Kalogerakis, N., Pintado, M.E., 2012. Bioconversion of oleuropein to hydroxytyrosol by lactic acid bacteria. World J. Microbiol. Biotechnol. 28, 2435–2440.
Sarroukh, R., Goormaghtigh, E., Ruysschaert, J.M., Raussens, V., 2013. ATR-FTIR: a "rejuvenated" tool to investigate amyloid proteins. Biochim. Biophys. Acta Biomembr. 1828, 2328–2338.
Schaffer, S., Müller, W.E., Eckert, G.P., 2010. Cytoprotective effects of olive mill wastewater extract and its main constituent hydroxytyrosol in PC12 cells. Pharmacol. Res. 62 (4), 322–327.
Serra, A., Rubió, L., Borràs, X., Macià, A., Romero, M.P., Motilva, M.J., 2012. Validation of determination of plasma metabolites derived from thyme bioactive compounds by improved liquid chromatography coupled to tandem mass spectrometry. J. Chromatogr. B Anal. Technol. Biomed. Life Sci. 905, 75–84.
Silva, S., Gomes, L., Leitão, F., Coelho, A.V., Vilas Boas, L., 2006. Phenolic compounds and antioxidant activity of Olea europaea L. Fruits and leaves. Food Sci. Technol. Int. 12 (5), 385–396.
Söldner, C.A., Sticht, H., Horn, A.H.C., 2017. Role of the N-terminus for the stability of an amyloid-β fibril with three-fold symmetry. PLoS One 12 (10), e0186347.
Souillac, P.O., Uversky, V.N., Fink, A.L., 2003. Structural transformations of oligomeric intermediates in the fibrillation of the immunoglobulin light chain LEN. Biochemistry 42 (26), 8094–8104.
Stefani, M., Rigacci, S., 2013. Protein folding and aggregation into amyloid: the interference by natural phenolic compounds. Int. J. Mol. Sci. 14, 12411–12457.
Taniguchi, S., Suzuki, N., Masuda, M., Hisanaga, S., Iwatsubo, T., Goedert, M., Hasegawa, M., 2005. Inhibition of heparin-induced tau filament formation by phenothiazines, polyphenols, and porphyrins. J. Biol. Chem. 280, 7614–7623.
Urbanc, B., Betnel, M., Bitan, G., 2011. Structural basis for Aβ1–42 toxicity inhibition by Aβ C-terminal fragments: discrete molecular dynamics study. J. Mol. Biol. 410, 316–328.
Valls-Pedret, C., Lamuela-Raventós, R.M., Medina-Remón, A., Quintana, M., Corella, D., Pintó, X., Martínez-González, M.Á., Estruch, R., Ros, E., 2012. Polyphenol-rich foods in the mediterranean diet are associated with better cognitive function in elderly Subjects at high cardiovascular risk. J. Alzheimer's Dis. 29 (4), 773–782.
Virmani, A., Pinto, L., Binienda, Z., Ali, S., 2013. Food, nutrigenomics, and neurodegeneration — neuroprotection by what you eat!. Mol. Neurobiol. 48, 353–362.
Vissers, M.N., Zock, P.L., Roodenburg, A.J., Leenen, R., Katan, M.B., 2002. Olive oil phenols are absorbed in humans. J. Nutr. 132 (3), 409–417.
Volpicelli-Daley, L.A., Luk, K.C., Patel, T.P., Tanik, S.A., Riddle, D.M., Stieber, A., Meaney, D.F., Trojanowski, J.Q., Lee, V.M., 2011. Exogenous α-synuclein fibrils induce Lewy body pathology leading to synaptic dysfunction and neuron death. Neuron 72, 57–67.
Wälti, M.A., Ravotti, F., Arai, H., Glabe, C.G., Wall, J.S., Böckmann, A., Güntert, P., Meier, B.H., Riek, R., 2016. Atomic resolution structure of a disease-relevant Abeta(1 − 42) amyloid fibril. Proc. Natl. Acad. Sci. U.S.A. 113, E4976–E4984.
Wang, H., Duennwald, M.L., Roberts, B.E., Rozeboom, L.M., Zhang, Y.L., Steele, A.D., Krishnan, R., Su, L.J., Griffin, D., Mukhopadhyay, S., Hennessy, E.J., Weigele, P., Blanchard, B.J., King, J., Deniz, A.A., Buchwald, S.L., Ingram, V.M., Lindquist, S., Shorter, J., 2008. Direct and selective elimination of specific prions and amyloids by 4,5-dianilinophthalimide and analogs. Proc. Natl. Acad. Sci. U.S.A. 105, 7159–7164.
Wu, L., Velander, P., Liu, D., Xu, B., 2017. Olive component oleuropein promotes β-cell insulin secretion and protects β-cells from amylin amyloid-induced cytotoxicity. Biochemistry 56, 5035–5039.
Yang, F., Lim, G.P., Begum, A.N., Ubeda, O.J., Simmons, M.R., Ambegaokar, S.S., Chen, P.P., Kayed, R., Glabe, C.G., Frautschy, S.A., Cole, G.M., 2005. Curcumin inhibits formation of amyloid beta oligomers and fibrils, binds plaques, and reduces amyloid in vivo. J. Biol. Chem. 280, 5892–5901.
Zafra-Gómez, A., Luzón-Toro, B., Capel-Cuevas, S., Morales, J.C., 2011. Stability of hydroxytyrosol in aqueous solutions at different concentration, temperature and with different ionic content: a study using UPLC-MS. Food Nutr. Sci. 2, 1114–1120.
Zhang, S., Liu, H., Yu, H., Cooper, G.J., 2008. Fas-associated death receptor signaling evoked by human amylin in islet beta-cells. Diabetes 57 (2), 348–356.